Blueshift in optical band gap in nanocrystalline Zn1−xCaxO films deposited by sol-gel method

Kamakhya Prakash Misra, R. K. Shukla, Atul Srivastava, and Anchal Srivastava

Citation: Appl. Phys. Lett. **95**, 031901 (2009); doi: 10.1063/1.3184789
View online: http://dx.doi.org/10.1063/1.3184789
View Table of Contents: http://apl.aip.org/resource/1/APPLAB/v95/i3
Published by the American Institute of Physics.

Blueshift in optical band gap in nanocrystalline $Zn_{1-x}Ca_xO$ films deposited by sol-gel method

Kamakhya Prakash Misra, R. K. Shukla, Atul Srivastava, and Anchal Srivastava[a)]
Department of Physics, University of Lucknow, Lucknow 226007, India

(Received 30 April 2009; accepted 28 June 2009; published online 20 July 2009)

A blueshift in the optical band gap of nanocrystalline $Zn_{1-x}Ca_xO$ thin films has been obtained. A 12.72% enhancement in the band gap of ZnO thin films has been obtained using Ca dopant for the first time. The band gap widens from 3.38 to 3.81 eV as the Ca concentration increases from $x=0$ to $x=0.15$. The films are deposited by sol-gel method and have a hexagonal wurtzite phase with no indication of calcium. Grain size lies in the range of 12–92 nm. Atomic force micrographs indicate much smaller rms surface roughness showing significantly smooth surfaces. © *2009 American Institute of Physics*. [DOI: 10.1063/1.3184789]

Band gap engineering of nanocrystalline ZnO films opens a gateway to optical and electronic nanodevices. Besides being environment friendly, biocompatible,[1] and versatile material for several applications,[2–7] ZnO is a promising material for transparent photonics viz. short wavelength optoelectronic devices due to its large exciton binding energy (60 meV) and wide direct band gap (3.37 eV) at room temperature. For smooth variation in band gap, the change in anions and cations in ZnO by isoelectronic impurities is important.[8] Substitution of Zn by Cd and Mg modifies the optical band gap of ZnO films toward lower and higher energies, respectively, and is reported abundantly in literature.[9–11] Different deposition techniques like pulsed laser deposition,[3,12] spin coating,[10,13,14] spray pyrolysis,[5,15] metal-organic chemical-vapor deposition,[16] etc. have been used to obtain such films. However, the effect of alloying of Ca with ZnO remains to be investigated.

Here we present hitherto unreported engineering of optical band gap in nanocrystalline ZnO films using Ca dopant. In this letter we report the synthesis and optical band gap variation in $Zn_{1-x}Ca_xO$ with $x=0-0.15$. Incorporation of Ca in ZnO leads to a decrease in average atomic number and is therefore expected to result in blueshifting[17] in the absorption edge. The x dependent structural, surface, and optical transmission properties are also reported. Regular granular growth of the films has been seen using atomic force microscopy (AFM). Here the films have been deposited using sol-gel spin coating method.

Prior to film deposition, the substrate slides of BK7 glass are properly cleaned in an ultrasonic cleaner using methanol, acetone, and de-ionized water.

The precursor for undoped films is prepared by obtaining 0.1*M* solution of zinc acetate dihydrate (99.9% pure, S-D fine chemicals) in isopropanol (99.9% pure, Ranbaxy chemicals) and diethanolamine (99.9% pure, Ranbaxy chemicals). The mixture is magnetically stirred at room temperature for 30 min to get a homogeneous solution. To this solution, appropriate volumes of 0.1 molar solutions of calcium nitrate tetrahydrate (98% pure, S-D fine chemicals) in ethanol (99.9% pure, Shymlakhs International) is added to obtain calcium doping of 5, 10, and 15 at %. This solution is again stirred for 30 min. Both the undoped and doped solutions are aged for one month. The precursor solutions thus obtained are spin coated on separate cleaned glass slides. Spinning speed is kept at 3000 rpm while the spinning time is 30 s. After each coating, the sample is heated from room temperature to 500 °C at a rate of 10 °C/min and then cooled back to room temperature. The process is repeated ten times for obtaining appreciable thickness. The precursor films thus obtained are annealed at 500 °C for 2 h. Thus there are four samples prepared, i.e., thin films of undoped ZnO, ZnO:5 at % Ca, ZnO:10 at % Ca, and ZnO:15 at % Ca. Here these samples are referred to as samples 1, 2, 3, and 4. All the samples are transparent on visual inspection.

The x-ray diffraction patterns for all the samples (see Fig. 1) have been recorded by x-ray diffractometer (Thermoelectron ARL X'tra) for 2θ values ranging from 7° to 75° using Cu $K\alpha$ radiation ($\lambda=1.540\ 56$ Å). As seen in the figure, the films are polycrystalline with hexagonal wurtzite type structure.[18,19] Prominent peaks occur along the planes[4,10,15,18,20] (100), (002), and (101) for all the samples. None of the x-ray diffraction (XRD) patterns show any evidence of CaO phase. Using the background noise level as a reference, the (*hkl*) orientation parameter[21] $\gamma_{(hkl)}$ is calculated from the relative heights of the (100), (002), and (101) reflection peaks using the expression $\gamma_{(hkl)}=I_{(hkl)}/(I_{(100)}+I_{(002)}+I_{(101)})$. The values for $\gamma_{(hkl)}$ vary from 0.12 to 0.78

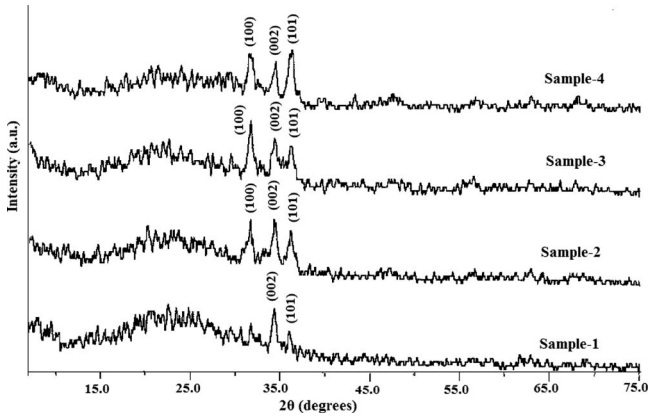

FIG. 1. XRD patterns of $Zn_{1-x}Ca_xO$ films. Samples 1, 2, 3, and 4 correspond to $x=0$, 0.05, 0.10, and 0.15.

[a)]Author to whom correspondence should be addressed. Electronic mail: asrivastava.lu@gmail.com.

TABLE I. Particle size as determined by DS formula and WH plot, and strain in the films.

Samples	t_{DS} (nm) (100)	t_{DS} (nm) (002)	t_{DS} (nm) (101)	t_{WH} (nm)	ε
1	⋯	18.51	26.78	2.47	9.1×10^{-2}
2	91.75	92.38	92.87	85.55	2.5×10^{-4}
3	7.24	19.26	21.16	1.18	2.0×10^{-1}
4	12.23	11.30	12.37	11.75	3.0×10^{-4}

indicating random orientation of the samples. The interplanar spacing for each of the crystallographic planes decreases as x in $Zn_{1-x}Ca_xO$ increases from 0 to 0.10, but for $x=0.15$ the trend reverses. The c-axis oriented peak, i.e., (002) peak occurs at $2\theta=34.324°$, 34.342°, 34.383°, and 34.247° for samples 1, 2, 3, and 4, respectively. Although small but continuous increment in 2θ values is observed with increasing Ca concentration up to $x=0.10$. The diffraction peak shifts back to a lower value of 2θ for further higher concentration of Ca, i.e., $x=0.15$. However, this leads to a very small change in c-lattice constant and hence in the volume of hexagonal cell. The particle size in the samples is estimated from the Debye–Scherrer's (DS) formula,

$$t_{DS} = \frac{k\lambda}{\beta \cos\theta},$$

where t_{DS} is the particle diameter, k is the Scherrer constant and is taken[16] equal to 1, λ is the wavelength of x-rays, and β is the full width at half maximum (FWHM) of x-ray diffraction peaks in radians. Particle size along each crystallographic plane as determined by the DS formula for all the samples is summarized in Table I.

In order to distinguish the effect of crystallite size-induced broadening and strain-induced broadening of FWHM of XRD profile, the Williamson and Hall (WH) plot[22] has been performed and shown in Fig. 2. The particle size and strain are obtained by comparing the trend line equation

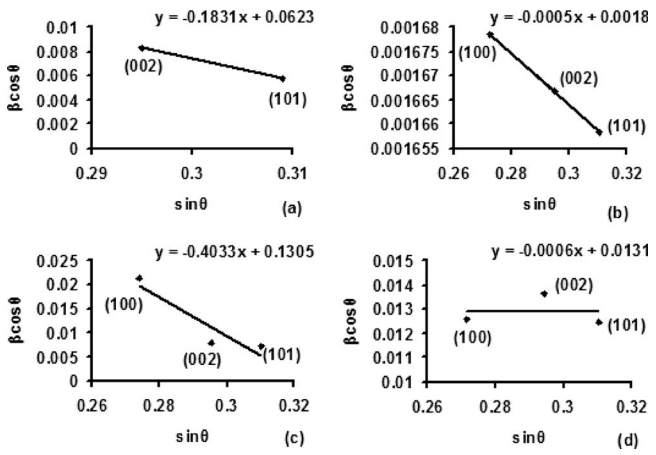

FIG. 2. WH plots for (a) $x=0$, (b) $x=0.05$, (c) $x=0.10$, and (d) $x=0.15$ for $Zn_{1-x}Ca_xO$ films.

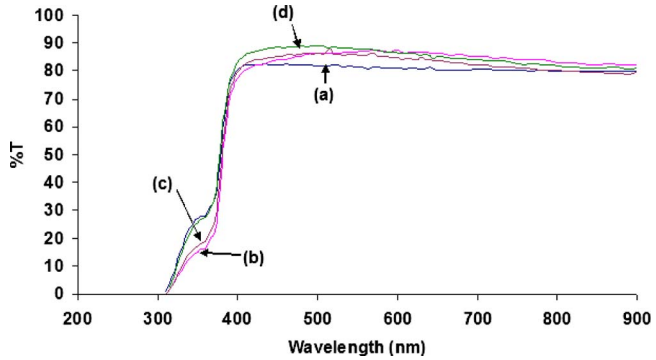

FIG. 3. (Color online) Transmission spectra for $Zn_{1-x}Ca_xO$ films. Curves a, b, c, and d correspond to samples 1 ($x=0$), 2 ($x=0.05$), 3 ($x=0.10$), and 4 ($x=0.15$), respectively.

$$\beta \cos\theta = \frac{C\lambda}{t_{WH}} + 2\varepsilon \sin\theta,$$

where t_{WH} is the particle size, ε is the strain, and C is the correction factor which is taken as 1. The strain and particle size thus determined are summarized in Table I. It is seen that the value of strain is much smaller, by an order of 3, for samples 2 and 4 as compared to samples 1 and 3. Therefore, for samples 2 and 4 the particle size obtained from DS formula nearly matches with that obtained by the WH plot. For samples 1 and 3 the particle size determined by the two methods are quite different indicating that for these samples, the broadening of FWHM is due to the strain existing in the films and not due to the particle size.

The optical transmission spectra is recorded using UV-visible spectrophotometer (Model No-108, Systronics, India) in the wavelength range 300–900 nm and is shown in Fig. 3. The measurements are taken in the wavelength scanning mode for normal incidence. From Fig. 3 it is seen that the films are highly transparent (80%–90%) in the infrared and visible region and absorption occurs near 300 nm. Transmission minimum is seen to blueshift with increasing Ca concentration. The absorption coefficient α is calculated from Beer's law $I=I_0e^{-\alpha d}$, where I is the transmitted intensity, I_0 is the incident intensity, and d is the thickness of the film. The absorption coefficient for direct band gap materials relates with optical band gap energy E_g according to the expression $\alpha=(h\nu-E_g)^{1/2}$, where h is the Planck's constant and ν is the frequency of incident photon. Intercept on the energy axis obtained by extrapolating the linear portion of the α^2 versus $h\nu$ plot (Fig. 4), gives the value of band gap E_g. Values of E_g thus determined are 3.38, 3.52, 3.79, and 3.81 eV for samples 1, 2, 3, and 4, respectively. Thus a 12.72% enhancement in the optical band gap of ZnO thin films has been obtained. This variation in band gap with dopant concentration x is shown in the inset of Fig. 4, linear fit to which follows the equation

$$E_g(x) = 3.12x + 3.391.$$

Thus, the optical band gap is tunable between 3.38 and 3.81eV for $0\leq x\leq 0.15$ for nanocrystalline $Zn_{1-x}Ca_xO$ thin films deposited on glass substrate using sol-gel spin coating technique. An enhancement of 12.64% in band gap is reported by Suchand Sandeep *et al.*[10] in $Zn_{1-x}Mg_xO$ hexagonal wurtzite thin films deposited by sol-gel method for $0\leq x\leq 0.20$. However, in the present study we have achieved the

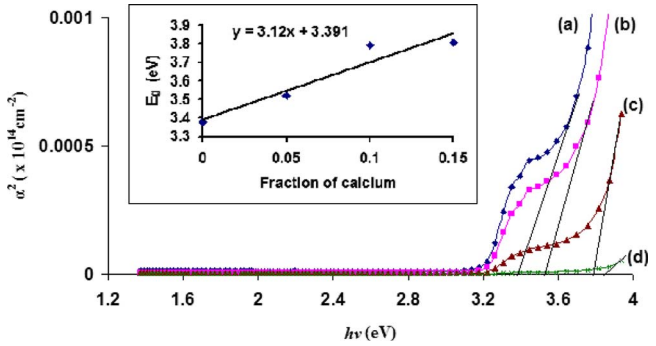

FIG. 4. (Color online) Plot of α^2 vs photon energy for $Zn_{1-x}Ca_xO$. Curves a, b, c, and d correspond to samples 1 (x=0), 2 (x=0.05), 3 (x=0.10), and 4 (x=0.15), respectively. The inset shows variation in band gap with Ca concentration.

enhancement with a comparatively smaller amount of dopant. The linear variation in band gap with x has also been reported in semiconductor alloy $Ge_{1-x}Si_x$.[21,23,24] Here the band gap has been found to increase with increasing concentration of the lighter cation in accordance with the report of Chelikowsky and Cohen,[17] which says that the optical band gap decreases with a heavier cation.

Surface topology of the films has been determined by AFM. AFM images are showing regular granular growth of thin films on the substrate. Figure 5 shows the three-dimensional AFM images of the undoped and Ca-doped ZnO films. The surface of undoped ZnO comprises of sharply pointed grain outgrowths. With an increase in Ca concentration in the $Zn_{1-x}Ca_xO$ films the surface becomes smoother as more and more grains club together. The three-dimensional images also show that with increasing Ca concentration, the area of the islands increase and they become broader leading to a decrease in surface roughness. The root-mean-square of the surface roughness of these films lies between 4 and 8 nm, indicating significantly smooth surfaces. The grain size obtained from AFM match with those obtained from XRD calculations.

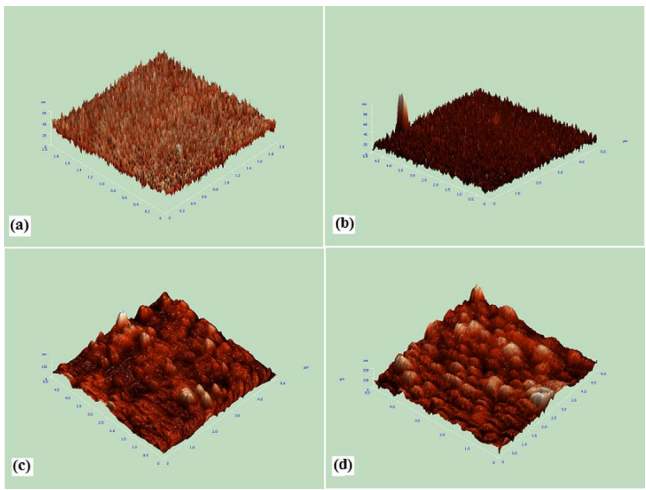

FIG. 5. (Color online) Three-dimensional AFM images for (a) x=0, (b) x=0.05, (c) x=0.10, and x=0.15 (d) for $Zn_{1-x}Ca_xO$ films.

In conclusion, a 12.72% enhancement and hence blueshift in the optical band gap in ZnO thin films has been obtained by Ca doping for the first time. $Zn_{1-x}Ca_xO$ thin films have been deposited on BK7 glass substrate by sol-gel spin coating technique. All the samples with different Ca concentration are hexagonal wurtzite nanocrystalline thin films with random orientation. The band gap of the films increases from 3.38 to 3.81 eV with the Ca concentration increasing from x=0 to x=0.15. This result is similar to the phenomenon in the semiconductor alloys. The result indicates that the tuning of the optical band gap can be achieved by controlling the Ca concentration in $Zn_{1-x}Ca_xO$ nanocrystalline films. This has potential application in fabrication of light-emitting devices.

Financial assistance from University Grants Commission, New Delhi, India vide Project no. F.No. 33-25/2007(SR) and its Special Assistance Programme is gratefully acknowledged. Authors thank Mr. C. Periasamy, TA, Institute of Technology, BHU, Varanasi, for performing AFM.

[1] J. G. Lu, Y. Z. Zhang, Z. Z. Ye, Y. J. Zeng, J. Y. Huang, and L. Wang, Appl. Phys. Lett. **91**, 193108 (2007).
[2] H. Kim, C. M. Gilmore, J. S. Horwitz, A. Pique, H. Murata, G. P. Kushto, R. Schlaf, Z. H. Kafafi, and D. B. Chrisey, Appl. Phys. Lett. **76**, 259 (2000).
[3] R. K. Shukla, A. Srivastava, A. Srivastava, and K. C. Dubey, J. Cryst. Growth **294**, 427 (2006).
[4] S. Dixit, A. Srivastava, A. Srivastava, and R. K. Shukla, J. Appl. Phys. **102**, 113114 (2007).
[5] D. Mishra, A. Srivastava, A. Srivastava, and R. K. Shukla, Appl. Surf. Sci. **255**, 2947 (2008).
[6] Ya. I. Alivov, E. V. Kalinina, A. E. Cherenkov, D. C. Look, B. M. Ataev, A. K. Omaev, M. V. Chukichev, and D. M. Bagnall, Appl. Phys. Lett. **83**, 4719 (2003).
[7] T. Yatsui, J. Lim, M. Ohtsu, S. J. An, and G.-C. Yi, Appl. Phys. Lett. **85**, 727 (2004).
[8] B. K. Meyer, A. Polity, B. Farangis, Y. He, D. Hasselkamp, Th. Kramer, and C. Wang, Appl. Phys. Lett. **85**, 4929 (2004).
[9] M. Lorenz, E. M. Kaidashev, A. Rahm, Th. Nobis, J. Lenzner, G. Wagner, D. Spemann, H. Hochmuth, and M. Grundmann, Appl. Phys. Lett. **86**, 143113 (2005).
[10] C. S. Suchand Sandeep, R. Phillip, R. Satheeshkumar, and V. Kumar, Appl. Phys. Lett. **89**, 063102 (2006).
[11] T. Makino, Y. Segawa, M. Kawasaki, A. Ohtomo, R. Shiroki, K. Tamura, T. Yasuda, and H. Koinuma, Appl. Phys. Lett. **78**, 1237 (2001).
[12] J.-L. Zhao, X.-M. Li, J.-M. Bian, W.-D. Yu, and X.-D. Gao, J. Cryst. Growth **276**, 507 (2005).
[13] Y. Cao, L. Miao, S. Tanemura, M. Tanemura, Y. Kuno, and Y. Hayashi, Appl. Phys. Lett. **88**, 251116 (2006).
[14] H.-C. Cheng, C.-F. Chen, and C.-Y. Tsay, Appl. Phys. Lett. **90**, 012113 (2007).
[15] J. L. van Heerden and R. Swanepoel, Thin Solid Films **299**, 72 (1997).
[16] S. T. Tan, B. J. Chen, X. W. Sun, W. J. Fan, H. S. Kwok, X. H. Zhang, and S. J. Chua, J. Appl. Phys. **98**, 013505 (2005).
[17] J. R. Chelikowsky and M. L. Cohen, Phys. Rev. B **14**, 556 (1976).
[18] S. Ilican, Y. Caglar, M. Caglar, and B. Demirci, J. Optoelectron. Adv. Mater. **10**, 2592 (2008).
[19] Y. Zhang, B. Lin, X. Sun, and Z. Fu, Appl. Phys. Lett. **86**, 131910 (2005).
[20] H. Sawada, R. Wang, and A. W. Sleight, J. Solid State Chem. **122**, 148 (1996).
[21] Y. W. Li, J. L. Sun, X. J. Meng, J. H. Chu, and W. F. Zhang, Appl. Phys. Lett. **85**, 1964 (2004).
[22] G. K. Williamson and W. H. Plot, Acta Metall. **1**, 22 (1953).
[23] E. R. Johnson and S. M. Christian, Phys. Rev. **95**, 560 (1954).
[24] D. Stroud and H. Ehrenreich, Phys. Rev. B **2**, 3197 (1970).